

Density dependence of electron scattering at low density

D. W. Snoke*

The Aerospace Corporation, P.O. Box 92957, Los Angeles, California 90009-2957

(Received 19 May 1994)

Several recent experiments have measured the rates of momentum relaxation and energy relaxation due to carrier-carrier scattering in GaAs as a function of density in three dimensions and in two dimensions. This paper examines the power laws for the density and temperature dependence of these rates based on the Boltzmann equation for electron-electron scattering, from both analytical arguments and numerical calculations. The experimental scaling with density is deduced for three-dimensional scattering over four orders of magnitude of density variation and two-dimensional scattering over two orders of magnitude. The effects of frequency-dependent terms in the random-phase approximation for the dielectric function are taken into account, as well as the effects of electron-hole scattering.

I. INTRODUCTION

In the past few years, a number of experiments have probed the rate of scattering of free carriers in semiconductors, primarily free conduction-band electrons in GaAs, as a function of electron density.^{1,8} Extensive data now exist on the rate of electron-electron scattering at the conduction band minimum in bulk GaAs in the range 10^{12} – 10^{18} cm^{-3} , six orders of magnitude of density variation. In addition, similar data from two-dimensional quantum wells of GaAs now exist over two orders of magnitude of density. The beauty of these experiments is that, although the *absolute* rate of scattering at a given density is difficult to determine, the *relative change* of the carrier-carrier scattering rate as density varies can be measured extremely accurately. Measuring the rate of carrier-carrier scattering in absolute units requires, first, a measure of the absolute carrier density and, second, knowledge of the absolute rate of scattering due to all other processes. An absolute measure of carrier density requires knowing the quantum efficiency of conversion of laser photons to carriers as well as the excited volume of carriers, both of which are difficult to measure to better than a factor of 2 uncertainty. Assuming that both of these are constant, however, the change in density of free carriers depends simply on the change in the laser intensity used to create them, which can be measured very accurately. The change in scattering rate with density can be assumed to be entirely due to carrier-carrier scattering, since the rates of electron-phonon scattering and electron-impurity scattering are essentially constant at low density. Therefore these experiments give a very clean test of theories of charged-carrier scattering.

Although complicating factors exist, such as screening of the electron-phonon interaction, elastic and inelastic scattering with carriers trapped at impurities and defects, and valence-band anisotropy, the theory governing these measurements to a large degree involves only the pure electron-electron Coulomb scattering matrix el-

ement, since scattering of electrons with each other via this process occurs much faster than all other processes, in most experimental conditions. The theory of Coulomb scattering is filled with difficulties however, and interpretation of past experiments has been subject to a sense of ambiguity, that no adequate theory for Coulomb scattering exists which covers all these densities and temperatures. This ambiguity stems from two inherent problems with Coulomb scattering: (i) unscreened Coulomb scattering has divergent cross section, and therefore care must be taken to use a valid theory of screening, and (ii) solution of the full Boltzmann equation, which gives the evolution of the particle distribution in time, is numerically intensive, and therefore numerous approximations of varying degrees of validity have been made.

Successful resolution of these questions would have application not only to hot carrier scattering in semiconductors, but also to plasma physics on large scales. Direct measurements of the rate at which electrons obtain a thermal distribution following a perturbation are scarce. Because free electrons can be “created” in a nonthermal distribution nearly instantaneously in a semiconductor by a laser pulse, however, and can be monitored optically thereafter, measurements in semiconductors may in fact be the most direct way of supplying this information for plasma physics.

In previous publications,^{7,9} I have presented a formalism for numerically solving the Boltzmann equation for Coulomb scattering of carriers, specifically as related to measurements of electron-electron scattering on picosecond time scale in bulk GaAs at ultralow densities.^{6,7} A number of questions, however, have remained regarding the density and temperature dependence of the scattering. In this publication, I discuss these dependences as related to a variety of experiments and I address specifically two other studies of electron-electron scattering at higher density, namely, a recent study of electron energy relaxation in two-dimensional (2D) and 3D GaAs (Ref. 5) and an earlier study of dephasing of electrons in 2D and 3D GaAs.^{1,2}

II. WRITING DOWN THE BOLTZMANN EQUATION

A. Electron-electron scattering

We begin by examining only electron-electron scattering in a spherical band, e.g., the GaAs conduction band at zone center. As discussed at the end of this section, the theory for electron-electron scattering can be generalized to apply to electron-hole scattering as well.

Simulations of the evolution of an electron gas scattering are based on first-order time-dependent perturbation theory, which according to the golden rule gives the rate of change of the occupation number f of a state \vec{k}_1 as

$$\begin{aligned} \frac{\partial f(\vec{k}_1)}{\partial t} = & \frac{2\pi}{\hbar} \sum_{\vec{k}_2, \vec{k}_1'} |M_{121'2'}|^2 \\ & \times \delta[E(\vec{k}_1) + E(\vec{k}_2) - E(\vec{k}_1') - E(\vec{k}_2')] \\ & \times [f_1' f_2' (1 - f_1)(1 - f_2) \\ & - f_1 f_2 (1 - f_1')(1 - f_2')]. \end{aligned} \quad (1)$$

As shown in numerous works, including Ref. 7, the relaxation-time approximation, which assumes a constant matrix element $M_{121'2'}$, i.e., a single relaxation time for all particles, gives a completely inadequate description of the evolution of a charged gas. The matrix element $M_{121'2'}$ for charged particle scattering depends strongly on the momentum and energy of the particles, according to

$$M_{121'2'} = \frac{1}{V} \frac{4\pi e^2}{\epsilon(K, \omega) K^2}, \quad (2)$$

where $K = |\vec{k}_1 - \vec{k}_1'|$ is the momentum exchanged in the two-body collision and $\hbar\omega$ is the energy exchanged. The dielectric constant $\epsilon(K, \omega)$ must be obtained from many-body calculations of varying degrees of approximation for the polarizability of the system.¹⁰ Most numerical studies of carrier-carrier scattering have used the quasistatic approximation for charged-particle scattering

$$\epsilon(K, 0)/\epsilon_\infty = \left(1 + \frac{q_0^2}{K^2}\right), \quad (3)$$

where q_0 is the quasistatic Debye-Hückel screening parameter, given by

$$q_0^2 = -\frac{4\pi e^2}{\epsilon_\infty} \sum_{\vec{k}} \frac{\partial f[E(\vec{k})]}{\partial E}, \quad (4)$$

where $f(E)$ is the instantaneous particle occupation number and ϵ_∞ is the high-frequency dielectric constant of the material. The distribution $f(E)$ is given by the Fermi-Dirac distribution when the distribution is thermalized, which is identical to a Maxwell-Boltzmann distribution for a low density electron gas. When a Maxwell-Boltzmann distribution is used in (4), the result

$$q_0^2 = \frac{4\pi e^2 n}{\epsilon_\infty k_B T} \quad (5)$$

is obtained, where n is the electron density. As reported in Ref. 9, when the distribution $f(E)$ is Gaussian instead of Maxwellian, the value of q_0^2 is approximately a factor of 3 lower than (5). It is therefore important to calculate q_0 from (4) using the instantaneous distribution of the electrons in a simulation instead of assuming a constant q_0 .¹¹

Numerical studies of electron-electron scattering have tended to use (2) and (3), i.e.,

$$M^2(K) = \frac{1}{V^2} \frac{16\pi^2 e^4 / \epsilon_\infty^2}{(K^2 + q_0^2)^2} \quad (6)$$

for the square of the scattering matrix element, primarily because it is simple to calculate. This quasistatic approximation is actually the $\omega \rightarrow 0$ and long-wavelength limit of the more general random-phase approximation (RPA) for the real part of the dielectric function ϵ ,¹²

$$\epsilon(K, \omega)/\epsilon_\infty = 1 - \frac{4\pi e^2}{K^2 V \epsilon_\infty} \sum_{\vec{k}} \frac{f(\vec{k} + \vec{K}) - f(\vec{k})}{E(\vec{k} + \vec{K}) - E(\vec{k}) + \hbar\omega}, \quad (7)$$

which predicts a resonance for $\omega \sim \omega_p = (4\pi e^2 n / \epsilon_\infty m)^{1/2}$, the plasmon energy of the gas. If $\omega \ll \omega_p$, the quasistatic approximation is valid. It turns out, however, that typical energies exchanged in the thermalization of an electron gas at low density are comparable to the plasmon energy, as seen in the following argument.

The energy exchange in a two-body collision is given by

$$\Delta E = \frac{\hbar^2 k^2}{2m} - \frac{\hbar^2 (\vec{k} - \vec{K})^2}{2m} = \frac{\hbar^2 (kK \cos \theta - K^2)}{2m}. \quad (8)$$

Figure 1 plots the probability of a collision, proportional to $M^2(K)$ given by (6), weighted by the energy exchanged $\Delta E \sim \hbar^2 kK$, assuming $K \ll k$. The function is strongly peaked at $K \sim q_0/2$, implying that the most important scattering events for the thermalization of the gas will have K with this value (thus justifying the as-

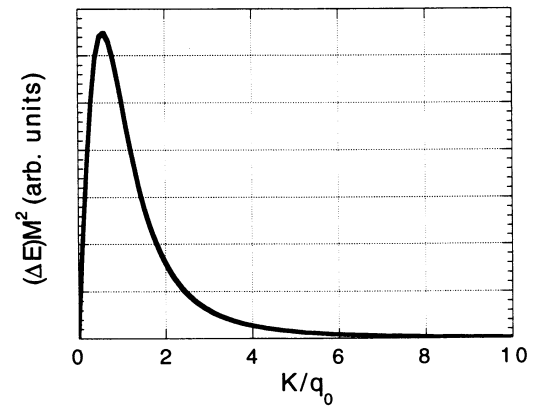


FIG. 1. The quasistatic Coulomb matrix element $M^2 = 1/(\epsilon K^2 + q_0^2)^2$ weighted by the average energy exchange $\Delta E \propto K$.

sumption $K \ll k$ for $q_0 \ll k$, the low-density limit). Taking $K = q_0/2$, then, and $\cos \theta$ at maximum, using the Debye formula (5) for q_0 , and taking $\hbar k$ at a typical thermal momentum gives

$$\frac{\Delta E}{\hbar\omega_p} = \frac{\hbar k(q_0/2)/m}{\omega_p} \quad (9)$$

$$= \frac{\sqrt{3mk_B T}}{2m} \sqrt{\frac{4\pi e^2 n}{\epsilon_\infty k_B T} \frac{\epsilon_\infty m}{4\pi e^2 n}} \quad (10)$$

$$= \frac{\sqrt{3}}{2}, \quad (11)$$

i.e., the plasmon energy is comparable to the energy exchanged in a typical collision, no matter what the density and temperature (in the nondegenerate regime.) We must therefore look more carefully at the effect of the plasmon resonance.

The RPA approximation (7) for ϵ can be written

$$\begin{aligned} \epsilon(K, \omega)/\epsilon_\infty &= 1 + \frac{q_{\text{RPA}}^2}{K^2} \\ &= 1 - \frac{4\pi e^2}{K^2 \epsilon_\infty} \int \frac{k^2 dk}{(2\pi)^3} d(\cos \theta) \frac{\delta f}{\frac{\delta E}{\delta k} + \frac{\hbar\omega}{\delta k}}, \end{aligned} \quad (12)$$

where $\delta k = \sqrt{(\vec{k} + \vec{K})^2} - k = K \cos \theta + K^2/2k \approx K \cos \theta$. Doing the integral over θ , assuming $E = \hbar^2 k^2/2m$, yields

$$\begin{aligned} \epsilon(\hbar\omega/K)/\epsilon_\infty &= 1 - \frac{4\pi e^2}{K^2 \epsilon_\infty} \int \frac{2k^2 dk}{(2\pi)^3} \frac{df}{dE} \\ &\times \left[1 + \frac{(\hbar\omega/K)}{4E(k)/k} \right. \\ &\times \left. \ln \left(\frac{|(\hbar\omega/K) - 2E(k)/k|}{(\hbar\omega/K) + 2E(k)/k} \right) \right], \end{aligned} \quad (13)$$

which is the same integral as in (4) except for a dimensionless logarithmic correction factor. Although the log function has an infinity at $\hbar\omega/K = \hbar^2 k/2m$, it is integrable. Figure 2(a) shows the screening parameter q_{RPA} for a test particle with momentum $\hbar\vec{k}'$, from (12) and (13), as a function of $E' \equiv 2m(\hbar\omega/K)^2/\hbar^2 \simeq \hbar^2(k'K \cos \theta'/K)^2/2m = E(k' \cos \theta')$, for a Maxwellian energy distribution of the particles. This figure shows that for most of the particles, the effect of the RPA correction is to reduce the static Debye screening parameter by a fraction which depends on the dimensionless ratio of the scattering particle energy to the average energy. A small fraction of the particles at high energy have a negative value of q_{RPA}^2 . In this case the matrix element diverges for $K = |q_{\text{RPA}}|$, which corresponds to plasmon emission. In the limit $k' \gg k$, i.e., $E' \gg k_B T$, the RPA correction factor in (13) is proportional to $1/E'$, which implies $q_{\text{RPA}} \propto E'^{-1/2}$, and therefore a divergence at energy $\hbar\omega = \hbar^2 k' \cos \theta' q_{\text{RPA}}/m = \text{const} = \hbar\omega_p$. This result is consistent with the conclusion of Pines and Bohm¹³

that only electrons with energy well above the average will emit plasmons.

Figure 2(b) shows the same calculation for a Gaussian energy distribution of the particles, which is a typical early nonthermal distribution generated by a laser. In this case, plasmon emission is prohibited for essentially all of the particles. These two calculations show that (i) the primary effect of taking the more general RPA approximation instead of the quasistatic approximation for a thermalized distribution is to reduce the average screening by a factor of 2 or so, i.e., to increase the scattering rate, while for a nonthermalized distribution the screening is slightly increased,¹⁴ and (ii) plasmon emission will not occur until the gas is substantially thermalized, when a number of electrons occupy the high-energy tail of the Maxwellian distribution. Since the RPA correction factor is dimensionless, however, the density and temperature dependencies of scattering rates deduced using the quasistatic approximation will remain correct.

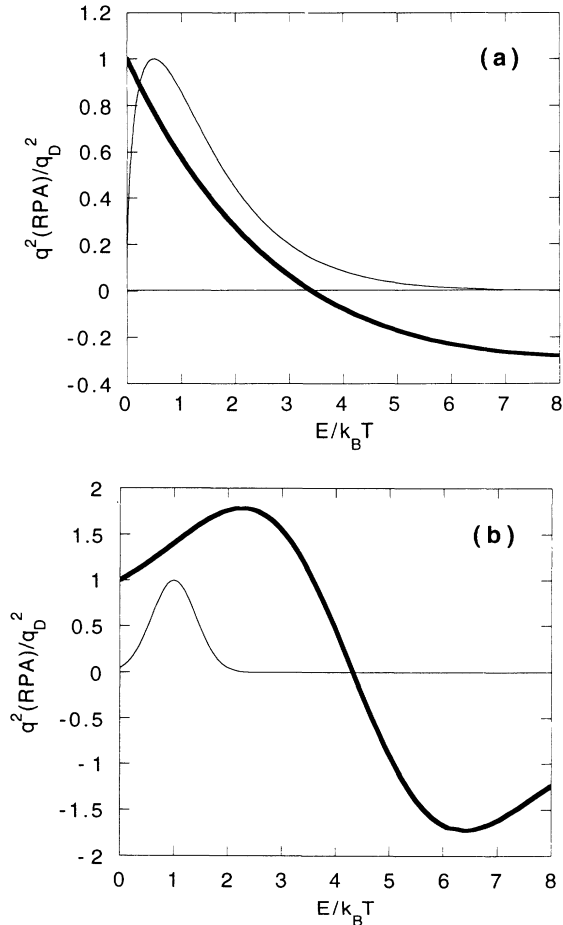


FIG. 2. (a) Heavy line: the screening wave vector q_{RPA} , defined in the text, relative to the quasistatic screening wave vector $q_D \equiv q_{\text{RPA}}(0)$, for the Maxwell-Boltzmann distribution shown as the light line. (b) Heavy line: the screening wave vector q_{RPA} relative to the quasistatic screening wave vector $q_D \equiv q_{\text{RPA}}(0)$, for the Gaussian distribution shown as the light line.

B. Electron-hole scattering

Scattering of electrons with holes involves essentially the same equations as in the above discussion. The Boltzmann equation is altered by the addition of a term equivalent to (1), but using f_h and E_h , the hole occupation number and energy, for the scattered particle with momentum \vec{k}_2 . In addition, the integrand must be multiplied by a factor $C(\vec{k}_2, \vec{k}_{2'})$ for the wave-function overlap of the anisotropic Bloch wave functions for the hole initial and final states \vec{k}_2 and $\vec{k}_{2'}$. As discussed, for example, by Wiley,¹⁵ for scattering of an electron with a hole near zone center which leaves the hole in the same (heavy or light hole) band, the matrix element (6) must be multiplied by a factor $(1 + 3 \cos^2 \chi)/4$, where χ is the angle between the incident and outgoing hole momenta; scattering of an electron with a hole which causes the hole to move from heavy hole to the light hole band or vice versa requires a multiplication factor of $3 \sin^2 \chi/4$. Since, as discussed above, Coulomb scattering at low density heavily favors scattering with low momentum exchange, the value of χ will typically be near zero, implying that scattering of an electron and hole which leaves the hole in the same band has essentially the same cross section as electron-electron scattering, while heavy hole-light hole conversion due to Coulomb scattering is nearly forbidden.¹⁶

When the presence of holes is taken into account in the screening, (7) is altered to¹²

$$\epsilon(K, \omega)/\epsilon_\infty = 1 - \frac{4\pi e^2}{K^2 V \epsilon_\infty} \sum_{\vec{k}, \alpha, \beta} C_{\alpha, \beta}(\vec{k}, \vec{k} + \vec{K}) \times \frac{f_\alpha(\vec{k} + \vec{K}) - f_\beta(\vec{k})}{E_\alpha(\vec{k} + \vec{K}) - E_\beta(\vec{k}) + \hbar\omega}, \quad (14)$$

where the subscripts $\alpha, \beta = e, l, h$ refer to conduction-electron, light-hole, and heavy-hole bands. Cross terms between the electron and hole bands are strongly suppressed by the large band-gap energy in the denominator, while cross terms between heavy and light hole bands are suppressed by the wave-function overlap factor discussed above, so that the screening becomes simply

$$\epsilon(K, \omega)/\epsilon_\infty = 1 + \frac{q_{ee, \text{RPA}}^2}{K^2} + \frac{q_{ll, \text{RPA}}^2}{K^2} + \frac{q_{hh, \text{RPA}}^2}{K^2}. \quad (15)$$

The three terms can be calculated separately from the instantaneous electron and hole distributions. In the quasistatic limit this leads to the conclusion that the total screening is given by

$$q_{\text{RPA}}^2 \propto \frac{n_e}{E_e} + \frac{n_l}{E_l} + \frac{n_h}{E_h}. \quad (16)$$

Particle mass does not enter. At early times following a laser pulse, when the hole population has much lower average energy than the free electron population, this would imply that screening due to holes will be *more* significant than screening due to other electrons. Figure 2 shows, however, that if the hole population is sub-

stantially colder than the electron population, the contribution of the holes to screening of the electron-electron scattering will be negative and comparable to or reduced in magnitude from the static value, partially canceling the contribution of electrons to the screening and thus *increasing* the scattering rate.

On the other hand, Kocevcar and co-workers¹⁷ have argued, on the basis of comparison to molecular dynamics calculations, that holes contribute far less to screening of the electron-electron scattering than indicated above. Their argument is that the holes cannot respond quickly enough to the motion of the electrons to adequately screen them, which is to say that the linear response assumption of the random-phase approximation breaks down on short time scales. This may be the case. Even if holes do contribute to screening as indicated above, however, the density dependence of the screening will not be affected at early times in experiments with band-to-band excitation, since the free hole density is proportional to the free electron density generated via this excitation method.

III. DENSITY DEPENDENCE OF MOMENTUM RELAXATION

A. Low-density regime

Since the presence of holes does not affect the density dependence of momentum relaxation in band-to-band excitation experiments, in the following we treat simply the electron-electron scattering in order to deduce the basic power laws. Taking the matrix element (6) in the quasistatic approximation (remembering that rates deduced this way will have to be multiplied by a dimensionless RPA correction factor), the total scattering rate out of some state \vec{k}_1 can be written in the low-density limit as

$$\frac{\partial f}{\partial t} d^3 k_1 = \frac{2\pi}{\hbar} \frac{gV^2}{(2\pi)^6} d^3 k_1 f(\vec{k}_1) \int d^3 k_2 d^3 k_{1'} d^3 k_{2'} f(\vec{k}_2) M^2 \times \delta(\vec{k}_1 + \vec{k}_2 - \vec{k}_{1'} - \vec{k}_{2'}) \times \delta(E_1 + E_2 - E_{1'} - E_{2'}), \quad (17)$$

where V is the volume and g is the band degeneracy.¹⁸ Since this expresses the rate of scattering out of some element of momentum space $d^3 k_1$, one can call this a momentum relaxation rate. It is common,¹⁹ however, to define the “momentum relaxation rate” using the above integral weighted by the factor $(1 - \cos \theta)$, where $\theta = \cos^{-1} \vec{k}_1 \cdot \vec{k}_{1'}/k_1 k_{1'}$ is the scattering angle, so that zero weight is given to elastic scattering which does not change the direction of the particles. Equation (17) expresses the “unweighted” momentum relaxation rate, or “total” scattering rate. Since dephasing of the coherent quantum wave functions of the particles is directly proportional to this rate,²⁰ it can also be called the “dephasing rate.”

Let us examine carefully the limit of this total scattering rate, or dephasing rate, at low density. Substituting the matrix element (6) into (17), and ensuring momentum conservation by substituting $\vec{k}_{1'} = \vec{k}_1 + \vec{K}$

and $\vec{k}_{2'} = \vec{k}_2 - \vec{K}$, one finds that (17) reduces to

$$\frac{1}{f(\vec{k}_1)} \frac{\partial f}{\partial t} d^3 k_1 = \frac{2\pi}{\hbar} \frac{g}{(2\pi)^6} d^3 k_1 \int d^3 k_2 f(\vec{k}_2) \frac{m}{\hbar^2} \frac{2e^4}{\epsilon_\infty^2} \frac{1}{k_r} \times \int_0^{2k_r} \frac{K dK}{(K^2 + q_0^2)^2}, \quad (18)$$

where $\vec{k}_r = (\vec{k}_1 - \vec{k}_2)/2$. The integral over K in (18) reduces to $1/2q_0^2$ in the limit $q_0 \ll k_r$, i.e., in the low-density limit. This just recovers the well-known total cross section for screened Coulomb scattering¹⁹ $\sigma_{\text{scatt}} \propto 1/k_r^2 q_0^2$.

Since the occupation number $f(\vec{k}_2)$ is proportional to the density n in the classical regime, and (4) implies that q_0^2 is proportional to n , this means that the total scattering rate (17) is *constant* at low density. (Numerical calculations of the same rate by a Monte Carlo method also find a constant total scattering rate as density is varied,²¹ in agreement with this analytical argument.) As discussed above, this does not change if RPA corrections are included. This expresses a fact similar to Olber's paradox for astrophysics—the $1/r^2$ potential implies that in an infinite system, although the strength of the interaction falls off at large distance, the number of particles at that distance increases as r^2 , so that the total contribution remains the same. This unweighted momentum rate does not tell the whole story about the electron gas thermalization however. The momentum relaxation rate weighted by $(1 - \cos \theta)$, which is related to transport measurements, does fall with density—in the low-density limit $k_1 \simeq k_1'$ and the term $(1 - \cos \theta) \approx \theta^2/2 \approx K^2/2k_1^2$ is proportional to q_0^2/T , which implies a momentum relaxation rate falling linearly with n . As discussed below, the energy relaxation rate also falls as density decreases.

B. High-density classical regime

This balance of q_0^2 increasing as n to cancel out the effect of increasing scattering partners cannot continue as density increases indefinitely. The screening length cannot be less than the average interparticle distance and in fact is not likely to be less than a few times the interparticle distance. The quasistatic formula (4) predicts a screening length decreasing as $n^{-1/2}$, however, while the interparticle separation decreases only as $n^{-1/3}$. At some point, the screening length will begin to follow the interparticle spacing, decreasing as $n^{-1/3}$. In this case, the total scattering rate (18) will depend on density as

$$\begin{aligned} \frac{1}{f(\vec{k})} \frac{\partial f}{\partial t} &\propto \frac{n}{q_0^2} \\ &\propto \frac{n}{n^{2/3}} \\ &\propto n^{1/3}. \end{aligned} \quad (19)$$

This is nearly exactly the density dependence seen in the study of dephasing of nondegenerate electrons in GaAs by Becker *et al.*¹ Since that dependence was seen for densities above 10^{17} cm^{-3} , while, as discussed below, the

energy-relaxation measurements of Kash⁵ show that the quasistatic approximation works well below that density, one can estimate the point at which the quasistatic approximation for the screening length (with RPA corrections) breaks down. We have, for a Gaussian distribution,

$$q_0 = \sqrt{\frac{3 \times 4\pi e^2 n}{\epsilon_\infty k_B T}} \sim \frac{n^{1/3}}{x}, \quad (20)$$

where x is some multiplier of the average interparticle distance. Assuming $T=300 \text{ K}$, a crossover at $n = 10^{17} \text{ cm}^{-3}$ implies that the Debye formula for the screening length breaks down when the screening length is less than $x \simeq 2$ times the interparticle spacing.

C. Two-dimensional scattering

Similar considerations can be made for momentum relaxation in two dimensions. In this case, the quasistatic matrix element for electron-electron scattering is^{22,23}

$$M^2(K) = \frac{1}{V^2} \frac{(2\pi e^2)^2}{(K + q_0)^2}, \quad (21)$$

where the screening parameter q_0 is given by

$$q_0 = -\frac{2\pi e^2}{\epsilon_\infty} \sum_{\vec{k}} \frac{\partial f[E(\vec{k})]}{\partial E}. \quad (22)$$

Writing down the equivalent integral in two dimensions as (18), one has

$$\begin{aligned} \frac{1}{f(\vec{k}_1)} \frac{\partial f}{\partial t} d^3 k_1 &\propto \frac{1}{k_r} \int_0^{2k_r} \frac{dK}{(K + q_0)^2} \\ &\rightarrow \frac{1}{k_r q_0} \quad \text{for } k_r \gg q_0. \end{aligned} \quad (23)$$

This yields the result that in the low-density limit, the unweighted momentum relaxation rate, or dephasing rate, is independent of density in two dimensions as well as in three dimensions. The scaling of the screening constant (22) will break down when screening length becomes comparable to the interparticle distance, as discussed above. In that case we have

$$\begin{aligned} \frac{1}{f(\vec{k})} \frac{\partial f}{\partial t} &\propto \frac{n}{q_0} \\ &\propto \frac{n}{n^{1/2}} \\ &\propto n^{1/2}, \end{aligned} \quad (24)$$

which is exactly the dependence seen in two dimensions in the study in GaAs by Bigot *et al.*² by the same experimental method used by Becker *et al.* for bulk GaAs.¹ The data of Bigot *et al.* give a lower bound on the crossover density for the breakdown of the quasistatic screening approximation, since an $N^{1/2}$ dependence was observed at all densities above 10^{10} cm^{-2} . Writing an equation like (20), using (22), assuming a breakdown of the qua-

sistatic screening at 10^{10} cm^{-2} , gives a value of x equal to 6 or 7, which is reasonable since screening in two dimensions is much less efficient than in three dimensions. No dephasing data exist for lower density. The energy-relaxation data of Kash⁵ for two dimensions cover the range 10^9 – 10^{11} cm^{-2} and are consistent with the scaling laws deduced here, as discussed below, but, as shown in that discussion, the energy relaxation rate in two dimensions does not depend on the screening length.

IV. DENSITY DEPENDENCE OF ENERGY RELAXATION

A. Three-dimensional scattering

We have seen that the total scattering rate is independent of density in the low-density limit. This comes about because even scattering of electrons at extremely large separation, with extremely low energy exchange, contributes to the total momentum relaxation rate. These scattering events contribute very little to the energy relaxation of the gas, however. An estimate of the energy relaxation rate, the rate at which a distribution broadens in energy width, can be obtained by weighting the integral (18) by the change in the energy separation of the two particles in a collision,

$$\begin{aligned} & \left| \left(\frac{\hbar^2 k_1^2}{2m} - \frac{\hbar^2 k_2^2}{2m} \right) - \left(\frac{\hbar^2 k_1'^2}{2m} - \frac{\hbar^2 k_2'^2}{2m} \right) \right| \\ &= \frac{\hbar^2}{2m} \left| k_1^2 - k_2^2 - [(\vec{k}_1 - \vec{K})^2 - (\vec{k}_2 + \vec{K})^2] \right| \\ &= \frac{\hbar^2}{m} \left| (\vec{k}_1 + \vec{k}_2) \cdot \vec{K} \right| = \frac{2\hbar^2 |\vec{k}_{c.m.} \cdot \vec{K}|}{m}, \end{aligned} \quad (25)$$

which is strictly proportional to K . As seen in Fig. 1, the Coulomb matrix element strongly favors scattering with $K = q_0/2$. Since, as shown in Sec. III A, the total scattering rate is proportional to $n/(\sqrt{E}q_0^2)$, the energy relaxation rate will have a density dependence given by this number times the average change in energy separation,

$$\frac{1}{\tau_E} \propto \frac{n}{\sqrt{E}q_0^2} k_{c.m.} q_0, \quad (26)$$

that is, $1/\tau_E \propto n^{1/2}$. This is essentially the density dependence seen in electron energy-relaxation experiments in bulk GaAs in the range 10^{15} – 10^{17} cm^{-3} by Kash.⁵

A more quantitative comparison of theory to the results of Kash can be made by solving the full Boltzmann equation (1) using the Coulomb matrix element with quasistatic screening. As shown in previous publications,^{24,9} when the distribution can be assumed isotropic, the total rate of change of the number of particles in an energy range $(E, E + dE)$ can be written as

$$\begin{aligned} \Gamma_0(E_1)dE &= (4\pi k_1^2 dk_1) \frac{df(k_1)}{dt} \\ &= \frac{2\pi}{\hbar} (8\pi^3) g \left(\frac{V}{(2\pi)^3} \right)^2 \left(\frac{dE}{d(k^2)} \Big|_{k=k_2'} \right)^{-1} k_1 dk_1 \int_0^\infty k_2 dk_2 \int_0^\infty k_1' dk_1' \int_{k_{low}}^{k_{high}} M^2(K) dK \\ &\quad \times \{ f(k_1') f(k_2') [1 - f(k_1)] [1 - f(k_2)] - f(k_1) f(k_2) [1 - f(k_1')] [1 - f(k_2')] \}, \end{aligned} \quad (27)$$

with $k_{high} = \min(k_1 + k_1', k_2 + k_2')/2$ and $k_{low} = \max(|k_1 - k_1'|, |k_2 - k_2'|)/2$; a similar equation is written for total scattering into the same energy range. (Umklapp processes are ignored.) Although we are interested in the energy relaxation, the integral is not weighted by the change in energy separation as discussed above, because the full solution of the Boltzmann equation keeps track of where all the electrons go; the rate of broadening in energy is obtained by a direct evaluation of the width of $f(E, t)$ as a function of time.

A typical solution of the Boltzmann equation simulating the experiment of Kash⁵ is shown in Fig. 3. In these experiments, a cold thermal distribution is created by an intense laser pulse preceding the probe pulse by 50 ps. This is represented by a Maxwell-Boltzmann distribution at 200 K in this model (half the LO phonon energy). Self-consistent quasistatic screening based on (4) using the instantaneous distribution $f(E)$ is incorporated in the calculation of $M(K)$, but RPA and hole-scattering corrections are not. The continuous function for the number of particles at a given energy $n(E)$ is represented in

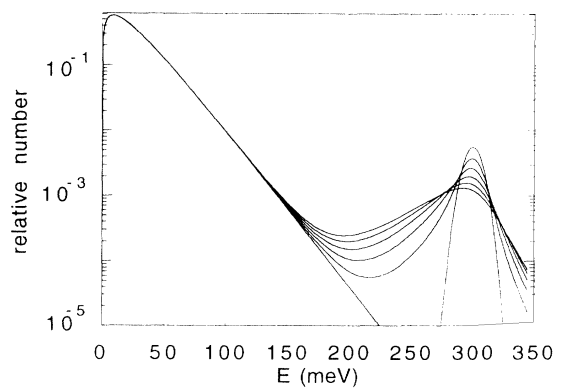


FIG. 3. Boltzmann-equation solution of a model of the Kash pulse-probe experiments (Ref. 5). The probe is assumed to be created instantaneously at $t = 0$ in a Gaussian distribution at $E = 300 \text{ meV}$ in the presence of a Maxwell-Boltzmann distribution with density $2 \times 10^{16} \text{ cm}^{-3}$. The curves correspond consecutively to the distribution at $t = 0, 0.35, 0.71, 1.09, 1.47, \text{ and } 1.82 \text{ ps}$.

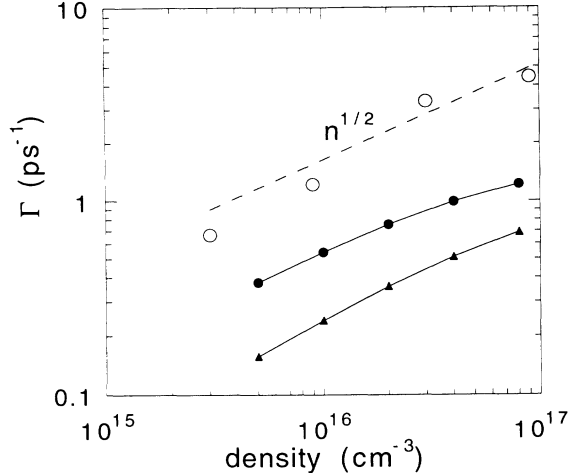


FIG. 4. Summary of the energy loss rate found by Kash (Ref. 5) (open circles), and calculated from the model shown in Fig. 3, as a function of density. Filled circles, initial probe energy width 10 meV; filled triangles, initial probe energy width 20 meV.

these calculations as a set of discrete values n_i for a set of energy channels $(E_i, E_i + dE_i) \equiv (E_i, E_{i+1})$, which approximates the continuous function well as long as the slope $[n(E_{i+1}) - n(E_i)]/dE_i$ is small. In addition, for the Boltzmann equation solution to be valid, the change in the matrix element for scattering to final states separated by dE must also be small, i.e., $dE \ll \hbar^2 k q_0 / 2m$.

Figure 4 shows a summary of the instantaneous energy relaxation rate, defined as

$$\Gamma_E = \left(\frac{1}{n} \sum_i \left| \frac{\partial n_i}{\partial t} \right| \right)_{\text{probe}}, \quad (28)$$

compared to the energy loss rate found by Kash,⁵ as a function of the electron density in the low-energy Maxwellian distribution generated by the pump pulse. As seen in this figure, the scaling of the rate with density in three dimensions seen by Kash is reproduced. The increase of the energy relaxation rate as $n^{1/2}$ falls off slightly at high density because Pauli exclusion becomes significant; the Kash data are not inconsistent with this. The energy relaxation rate depends on the initial energy width of the probe pulse, as discussed in Ref. 7; the upper curve in Fig. 4 (10 meV width) corresponds most closely to the experiments of Kash. Since the absolute value of the density in the experiments of Kash is certain only to within a factor of 2, and RPA and hole corrections are not included in the theory, a direct comparison of the absolute value of the thermalization rate as predicted by the model to that of experiment is not possible. Nevertheless, the model reproduces the energy relaxation rate found by Kash roughly within a factor of 2. The faster relaxation seen in the experiments can presumably be accounted for by including hole scattering and RPA effects, which increase the scattering rate but do not change the density dependence, as discussed in Sec. II.

Instead of defining the energy relaxation rate by the

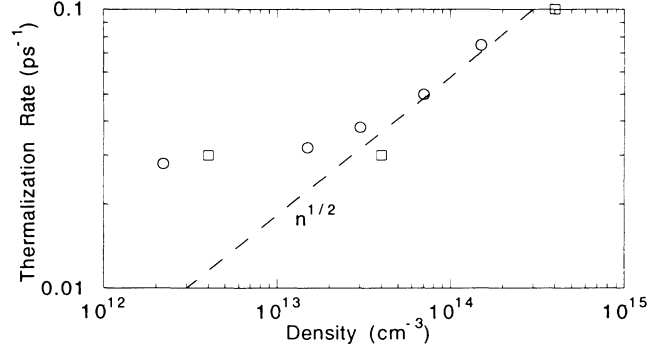


FIG. 5. Summary of the thermalization-rate data of Refs. 7 (open squares) and 8 (open circles).

time for a narrow (e.g., Gaussian) distribution to be depleted and broadened, as in the experiments of Kash, we can define a long-term “thermalization time” as the earliest time at which the entire electron distribution can be well fit by a Maxwell-Boltzmann distribution, $N(E) \propto E^{1/2} e^{-E/k_B T}$. Quantitatively, one can express this as the time at which $I(E)/E^{1/2}$, where $I(e)$ is the observed energy distribution, fits a straight line on a semilog plot with correlation of 90%. The experiments of Refs. 7 and 8 measure this time at low electron density; Fig. 5 shows a summary of the thermalization rates measured in these experiments. Since the “thermalization time” measures the rate of the change of the *shape* of a distribution, the energy relaxation rate (26) must be normalized by $k_B T$ to give the proper dependence on T ; instead of the weak $T^{1/2}$ dependence of (26), the thermalization time has the temperature dependence $T^{-1/2}$. The density dependence, however, is unchanged. As seen in Fig. 5, the thermalization rate scales approximately as $n^{1/2}$ at the highest densities, consistent with this argument and similar to the results of Kash.

This dependence was seen in the numerical calculations of Ref. 9 within the numerical uncertainties; however, that work argued for a constant rate of thermalization at low density on the basis of an analytical argument [Eq. (8) of Ref. 9] which used an improper weighting for the energy broadening. The constant rate of thermalization seen at extremely low densities in Refs. 7, 9 and 8 is still not understood. Reference 9 showed that the constant rate of thermalization cannot be due to phonon emission; recent work⁸ has confirmed the argument of Ref. 7 that it is not due to inelastic scattering with donors. The answer most likely lies in the fact that the threshold density for this effect is also the density at which the average interparticle spacing becomes comparable to the absorption length of the laser light in GaAs ($\sim 2 \mu\text{m}$) and therefore the screening becomes weaker and quasi-two-dimensional, even though the density of states of the electrons remains three dimensional.

B. Two-dimensional scattering

Just as in Sec. IV A, the density dependence of the energy relaxation rate in two dimensions can be found by

TABLE I. Density and temperature dependence of rates for electron-electron scattering.

	Dephasing	Energy relaxation	Thermalization
Low density			
3d	$T^{1/2}$	$n^{1/2}T^{1/2}$	$n^{1/2}T^{-1/2}$
2d	$T^{1/2}$	n	nT^{-1}
High density			
3d	$n^{1/3}T^{-1/2}$	$n^{2/3}$	$n^{2/3}T^{-1}$
2d	$n^{1/2}T^{-1/2}$	n	nT^{-1}

weighting the result for the total scattering rate. From Sec. III C, the energy relaxation rate in two dimensions is proportional to n/q_0 . This is weighted by the change in energy separation per collision, proportional to $\sqrt{\bar{E}}q_0$, to give an energy relaxation rate proportional to n .

At higher densities, when the screening length becomes comparable to the average interparticle separation, the same result is obtained because the energy relaxation rate does not depend on the screening length, in the above estimation. Therefore the results of Kash,⁵ which showed an energy relaxation rate proportional to n , are consistent with the results of Bigot *et al.*,² which found a dephasing rate proportional to $n^{1/2}$ in the same density range.

V. CONCLUSIONS

Table I summarizes the density and temperature dependence of the various rates discussed in this work, in two and three dimensions in both the low-density regime and the screening-limited regime. The electron gas is assumed nondegenerate in all cases—if the gas is degen-

erate, then Pauli exclusion will reduce the rate of increase at higher densities from these power laws or even cause rates to decrease with increasing density.

Although complicating factors due to holes and plasmons exist, these do not substantially affect the theoretical predictions for the density dependence of the scattering. The success of these calculations at deducing the observed power laws in a number of experiments shows that the density dependence of the scattering rates can be understood primarily in terms of the basic predictions for electron-electron scattering.

ACKNOWLEDGMENTS

I thank P. Supancic, K. El-Sayed, M. Kane, and J. Kash for helpful interactions. I thank W.W. Rühle and R. Hannak for permission to use the data of Fig. 5 as well as for useful interactions at all stages of this work. This work has been done as part of the Aerospace Sponsored Research program.

* Present address: Department of Physics and Astronomy, University of Pittsburgh, Pittsburgh, PA 15260.

¹ P.C. Becker, H.L. Fragnito, C.H. Brito Fork, J.E. Cunningham, J.E. Henry, and C.V. Shank, Phys. Rev. Lett. **61**, 1647 (1988).

² J.-Y. Bigot, M.T. Portella, R.W. Schoenlein, J.E. Cunningham, and C.V. Shank, Phys. Rev. Lett. **67**, 636 (1991).

³ T. Elsaesser, J. Shah, L. Rota, and P. Lugli, Phys. Rev. Lett. **66**, 1757 (1991).

⁴ J.A. Kash, Phys. Rev. B **40**, 3455 (1989).

⁵ J.A. Kash, Phys. Rev. B **48**, 18336 (1993).

⁶ D.W. Snoke, W.W. Rühle, Y.-C. Lu, and E. Bauser, Phys. Rev. Lett. **68**, 990 (1992).

⁷ D.W. Snoke, W.W. Rühle, Y.-C. Lu, and E. Bauser, Phys. Rev. B **45**, 10979 (1992).

⁸ R.M. Hannak and W.W. Rühle (unpublished).

⁹ D.W. Snoke, Phys. Rev. B **47**, 13346 (1993).

¹⁰ As discussed in Ref. 9, exchange effects can be ignored at low density; calculations by J. Collet, Phys. Rev. B **47**, 10279 (1993), indicated that these become significant at carrier densities above about 10^{17} cm⁻³ for hot (60 meV) electrons in GaAs.

¹¹ The effect of a peak versus a Maxwellian distribution on

electron scattering (specifically the emission of plasmons) has also been addressed by El Sayed *et al.*, Phys. Rev. B **47**, 10210 (1993).

¹² For example, G. Mahan, *Many-Particle Physics* (Plenum, New York, 1981).

¹³ D. Pines and D. Bohm, Phys. Rev. **85**, 338 (1952).

¹⁴ This conclusion has also been reached independently by M.G. Kane, K.W. Sun, and S.A. Lyon, Phys. Rev. B **50**, 7428 (1994).

¹⁵ J.D. Wiley, Phys. Rev. B **4**, 2485 (1971).

¹⁶ The result of calculations by J.F. Young *et al.*, Solid State Electron. **31**, 663 (1988), that intervalence band scattering can contribute substantially to carrier thermalization, is based on their choice of a relatively high carrier density and their use of the Debye static screening approximation for a Maxwellian distribution, which implies strong screening and, consequently, large-angle scattering.

¹⁷ U. Hohenester, P. Supancic, P. Kocevar, X.Q. Zhou, U. Lemmer, G.C. Cho, W. Kütt, and H. Kurz, Semicond. Sci. Technol. **7**, B176 (1992); U. Hohenester, P. Supancic, P. Kocevar, and L. Rota, in Proceedings of the Eighth Vilnius Symposium on Ultrafast Phenomena in Semiconductors [Lithuanian J. Phys. **32**, 117 (1992)]; U. Hohenester, P.

Supancic, P. Kocevar, X.Q. Xhou, W. Kütt, and H. Kurz, Phys. Rev. B **47**, 13 233 (1993).

¹⁸ Only one one factor of g is included here, in contrast to Refs. 7 and 9, since spin flip does not occur via Coulomb scattering—the density of final states is reduced.

¹⁹ For example, B.K. Ridley, *Quantum Processes in Semiconductors* (Clarendon, Oxford, 1988).

²⁰ D.C. Scott, R. Binder, and S.W. Koch, Phys. Rev. Lett.

69, 347 (1992).

²¹ P. Supancic and P. Kocevar (private communication).

²² K. El-Sayed, T. Wicht, H. Haug, and L. Bányai, Z. Phys. B **86**, 345 (1992).

²³ T. Ando, A.B. Fowler, and F. Stern, Rev. Mod. Phys. **54**, 437 (1982).

²⁴ D.W. Snoke and J.P. Wolfe, Phys. Rev. B **39**, 4030 (1989).